Atmos. Chem. Phys. Discuss., https://doi.org/10.5194/acp-2017-945
Manuscript under review for journal Atmos. Chem. Phys.
Discussion started: 15 December 2017

Atmospheric Chemistry and Physics Discussions

Sensitivity of Biogenic Volatile Organic Compounds Emissions to Leaf Area Index and Land Cover in Beijing

Hui Wang[1, 4], Qizhong Wu[1, 4], Hongjun Liu[2], Yuanlin Wang[3, 4], Huaqiong Cheng[1, 4], Rongrong Wang[1, 4], Lanning Wang [1, 4], Han Xiao[1, 4], Xiaochun Yang[1, 4]

[1]College of Global Change and Earth System Science, Beijing Normal University, Beijing 100875, China
[2]Department of Physics, Beijing Normal University, Beijing 100875, China
[3]State Key Laboratory of Atmospheric Boundary Layer Physics and Atmospheric Chemistry, Institute of Atmospheric Physics, Chinese Academy of Sciences, Beijing 100029, China
[4]Joint Center for Global Changes Studies, Beijing Normal University, Beijing 100875, China

Correspondence to: Qizhong Wu (wqizhong@bnu.edu.cn)

Abstract. The Beijing area has suffered from severe air quality pollution in recent years, including ozone pollution in summer. Except for the anthropogenic emissions inventory, understanding the local ozone pollution still requires the reliable biogenic emission inventory. The forest coverage rate rose from 20.6% to 35.8% during 1998-2013 in Beijing according to the National Forest Resource Survey (NFRS). In this study, we established a new high resolution biogenic volatile organic compounds (BVOCs) emission inventory in Beijing based on Model of Emission of Gases and Aerosols from Nature (MEGAN) v2.1 model with three independent leaf area index (LAI) products and three independent land cover products. The Global LAnd Surface Satellite (GLASS) LAI, Moderate-Resolution Imaging Spectroradiometer (MODIS) MCD15 LAI, GEOland (GEO) v2 LAI datasets, and the Finer Resolution Observation and Monitoring of Global Land Cover (FROM-GLC), MODIS MCD12Q1 PFT products and Climate Change Initiative Land Cover (CCI-LC) products are used to design five experiments, as E1-E5, to calculate and test the sensitivity of the model. Based on the meteorological conditions from Weather Forecasting and Research (WRF) model, this inventory is an hourly inventory with 3-km spatial resolution. The result shows: (1) According to the baseline estimation, the total amount of BVOCs emissions are 99.9 Gg for Beijing area. The estimated annual emissions of isoprene, monoterpenes, sesquiterpenes and other VOCs are 52.5 Gg, 11.1 Gg, 1.4 Gg and 34.9 Gg, respectively. (2) The BVOCs emissions have the significant seasonal variability, which the summer season contributes 76.6% of the total BVOCs emissions in Beijing, and the winter season only contributes 0.3% emissions due to the low temperature and near-zero biomass of deciduous trees. (3) The broadleaf tree, as the dominant contributor to the BVOCs emissions, accounts for 94.5% isoprene, 53.3% monoterpenes, 53.8% sesquiterpenes and 34.1% other VOCs. (4) The MODIS LAI lead to a 17.4% decline in BVOCs emissions because of the large mask area near the urban and water area. However, the GEO and GLASS LAI only led to a 1.0% difference of total BVOCs emissions even with different temporal updating frequency of LAI. (5) The difference of PFTs have an obvious effect on the spatial distribution and density of BVOCs emissions. The MODIS and CCI-LC land cover led to an approximate 5.0% and 26.0% decline in BVOCs emissions compared with the baseline estimation. (6) The estimation of local BVOCs emissions in this study is much higher than the previous studies, and the development of local forest is main

reason led to such the difference, thus implying that previous estimation of BVOCs in Beijing is underestimated and is not suitable for the current scene. In addition, further study will investigate and evaluate the effect of BVOCs on the local atmospheric environment through the regional chemistry transport model.

1. Introduction

The biogenic volatile organic compound (BVOC) plays a significant role in the atmospheric environment because of its large emission amount and high reactivity (Fuentes et al., 2000;Guenther et al., 1995). BVOCs can form secondary organic aerosol (SOA) (Claeys et al., 2004;Kavouras et al., 1998); meanwhile, it also affects tropospheric ozone (O_3) with the nitrogen oxides radicals(NO_X) (Fuentes et al., 2000;Seinfeld and Pandis, 2012). The BVOCs emissions are affected by meteorological conditions, including the radiation, temperature, and concentration of carbon dioxide (Arneth et al., 2007;Guenther et al., 2006;Guenther, 1993). As estimated by Guenther et al. (2012), the global total BVOCs flux is approximately 1000 Tg. Additionally, under the situation of climate change and global warming, the environmental conditions and anthropogenic activities would have an impact on the emission activities of BVOCs, which could lead to the relevant feedback on climate and human beings (Penuelas and Staudt, 2010). Under the background of global warming, as estimated by Stavrakou et al. (2014), the isoprene emissions in East Asia and China are increased by the positive trend of 0.2% yr^{-1} and 0.5% yr^{-1} respectively from 1979-2005. In addition, considering the severe air quality problem in China, addressing the contribution from natural and anthropogenic sources could benefit the strategies making for air quality control.

And as estimated by Klinger et al. (2002), the total amount of BVOCs emissions in China is about 21.0 Tg, and terpenoids is approximate 8.06 Tg, which is similar to the result (10.9 Tg) estimated by Tie et al. (2006). Since subtropical regions in China have the serious ozone pollution and abundant forests, multiple studies focused on the local biogenic emission and its potential effect on city air quality (Wang et al., 2011;Leung et al., 2010;Wang et al., 2013). As a typical city in North China, Beijing faces the severe ozone pollution in summer (Wang et al., 2006;Safieddine et al., 2016;Zhao et al., 2010). And the model and satellite results both indicate that the North China plain suffered relatively more severe O_3 pollution than the southern region in China in summer (Zhao et al., 2010;Safieddine et al., 2016). As a city encompassed by mountains and temperate forests, it is necessary to investigate and evaluate the impact of the biogenic sources on local air pollution. Previous studies have done some coarse calculations of local BVOCs emissions (Zhihui et al., 2003;Klinger et al., 2002), these estimations are for an earlier period (1998-2000), and the statistical data from the Nation Forest Resources Survey (NFRS) reported that the forest coverage rate in Beijing rose from 20.6% to 35.8% during 1998-2013. Meanwhile, the dominant tree species of the local forests are *Quercus* and *Populus*, which have high isoprene emission abilities (Zhihui et al., 2003). Therefore, a new high temporal and spatial resolution BVOCs emission inventory for the whole Beijing municipality in the current scene is needed to evaluate the natural effect on local air quality.

In this study, we present the new estimation of BVOC inventory of Beijing in 2013 based on the Model of Emission of Gases and Aerosols from Nature (MEGAN). In addition, we used multiple satellite datasets of leaf area index (LAI) and land cover (LC) products to discover the uncertainty of LAI and LC inputs. Sec. 2 introduces the models and datasets adopted in this study. In Sec. 3, we elaborate our results of the BVOCs emission inventory as well as the sensitivities of model to different satellite inputs. We present our conclusion and future work in Sec. 4.

2. Methodology

2.1 Model Description

The latest MEGAN v2.1 model is adopted to investigate local BVOCs emissions. The MEGAN model was developed to calculate the emissions of trace gases and aerosols from terrestrial ecosystems to the atmosphere, and it is widely used in studies on local air quality (Carlton and Baker, 2011;Geng et al., 2011) and global climate change (Emmons et al., 2010;Makkonen et al., 2012). The BVOCs emission rate in MEGAN is calculated by the following equation (Guenther et al., 2006):

$$\text{Emission} = [\varepsilon] \cdot [\gamma] \cdot [\rho]$$

where ε is a factor that accounts for the emission rates of different compounds in the standard canopy conditions, γ is an activity factor that accounts for the environmental variance, and ρ is a factor that accounts for the chemical and physical loss in the plant canopy layer.

2.1.1 Emission Factors

The standard emission rates in MEGAN adopts the canopy-scale emission factors (mg m^{-2} h^{-1}), which are converted from the measured leaf/branch-scale emission factors. The leaf/branch-scale emission factor, leaf mass per area (LMA, g m^{-2}) and the standard environmental factor were used to convert the leaf/branch-scale emission factors to canopy-scale emission factors (Leung et al., 2010;Guenther et al., 2006). In MEGAN, the ε can be described by either the specific trees species map or the plant function type (PFT) map (Guenther et al., 2006). In this study, we adopted six PFT species to explain the standard emission factors as follows: broadleaf trees, needleleaf trees, shrubs, crops, corn and grass. Moreover, we modified the standard emission factor of isoprene for every PFT according to the local field measurements from previous publications (Zhihui et al., 2003;Klinger et al., 2002). Based on the area data from the seventh NFRS, the area proportions of different tree species were used to weigh and calculate the emission factors of isoprenes for the PFTs mentioned above. Due to the lack of the measurements of emission factors in the local region, other VOC species adopted the default emission factors of MEGAN v2.1. Table 1 shows the original and adjusted standard emission factors of isoprenes, and the high area fraction (28.6%) of *Quercus* and *Populus* increased the emission factor of broadleaf trees from 10000 to 11736 μg/m^2·h.

2.1.2 Environmental activity factor

The environmental activity factor accounts for the effects of leaf age, canopy meteorological environment and soil moisture in MEGAN, and it can be expressed as:

$$\gamma = \gamma_{CE} \cdot \gamma_{age} \cdot \gamma_{SM}$$

where γ_{CE} accounts for the variation of the canopy meteorological conditions, γ_{age} describes the effect of the leaf age, and γ_{SM} explains the impact of the soil moisture.

The temperature and photosynthetically active radiation (PAR) are the main canopy meteorological factors that affect the BVOCs emission. The emission of isoprene is fully light- and temperature-dependent, and algorithms of isoprene emission conditions were described by Guenther et al. (2012). To monoterpene and sesquiterpene, approximately 10% monoterpene and 50% sesquiterpene were treated as light- and temperature-dependent, and the others are treated as temperature-dependent species in MEGAN (Sakulyanontvittaya et al., 2008). The moisture factor γ_{SM} is only considered for the isoprene emission. The corresponding canopy models are adopted to calculate the sunlit and shaded leaves temperature and light scattering of each PFT type (Guenther et al., 1999;Guenther et al., 2006). The details of the algorithms for isoprene and monoterpenes can be found in Guenther et al. (2012) and Sakulyanontvittaya et al. (2008).

2.2 Data & Simulation Description

In previous researches on estimating the BVOCs emission in Beijing (Zhihui et al., 2003;Klinger et al., 2002), the meteorological conditions were considered relatively simple. Zhihui et al. (2003) used the data from only one station to account for the meteorological conditions of the entire Beijing area, and the effect of the spatial variability of meteorological conditions on BVOCs emission was ignored. In this study, we used the mesoscale weather model to provide the meteorological conditions. Due to the lack of direct observations of canopy emission, we constrained the input conditions to discuss the sensitivity of emission inventory; thus, three different PFT and three LAI datasets are adopted to investigate the impact of inputs.

2.2.1 WRF Meteorological Simulation

The Weather Forecasting and Research (WRF) V3.3.1 (Skamarock et al., 2005) model was used to provide the meteorological conditions. The initialization field and boundary conditions for WRF are provided by the National Centers for Environmental Prediction (NCEP) FNL (Final) analysis datasets (https://rda.ucar.edu/datasets/ds083.2/). Three nested domains with 27-9-3 km spatial resolutions are adopted, and the finest grids covered Beijing are used for the inventory. The 48-h simulations were done day by day, and we considered the second day as the reasonable results. The hourly results were cut and merged to provide the whole year meteorological conditions for MEGAN.

The daily temperature (T2) simulated by WRF is primarily verified by the in situ data from 14 monitoring sites among the Beijing region. As shown in Table 2, the average mean error (ME), mean bias (MB), correlation coefficient (R) and root mean

square error (RMSE) of T2 are 2.78, -1.5, 0.96 and 3.4, respectively. The high R (0.96) indicates that the simulation catches the daily variation of temperature; however, there still exists a systematic cooling bias of -1.5°C. Figure 1 shows the location of all sites, and color indicates the MB of T2. Over all sites, Tong Zhou, Da Xing and Fang Shan have the most obvious underestimations of surface temperature with high negative biases of -4.84, -5.11 and -4.5, respectively. These sites are located in the suburban regions of Beijing where has been covered with the impervious layer, and the discrepancy between the real situation and old surface data in the WRF directly led to the cooling bias in these sites. Fortunately, the main contributor of BVOCs is the rural forest around Beijing, therefore, the simulation bias of the suburban regions could have little impact on the estimation of total BVOCs emission.

The downward shortwave radiation (DSW) is also validated with the in-situ data of the single station in Beijing. The R of the downward shortwave radiation is 0.51 and the MB of 56.79 indicates the overestimation of DSW. Such positive bias is mainly due to the lack of consideration of aerosol in the simulation, which would lead to the overestimation of BVOCs emission (Wang et al., 2011).

2.2.2 Satellite Datasets

The PFT or the LC datasets include the Finer Resolution Observation and Monitoring of Global Land Cover （FROM-GLC）(http://data.ess.tsinghua.edu.cn/), MODIS MCD12Q1 PFT products (https://lpdaac.usgs.gov/) and Climate Change Initiative Land Cover (CCI-LC) products (https://www.esa-landcover-cci.org/). Three kinds of LAI data products are adopted as the LAI inputs, including Global Land Surface Satellite (GLASS) LAI datasets (Xiao et al., 2014;Xiao et al., 2016) (http://glass-product.bnu.edu.cn/), Moderate-Resolution Imaging Spectroradiometer (MODIS) MCD15 LAI datasets (https://lpdaac.usgs.gov/) and Geoland (GEO) v2（http://land.copernicus.eu/） (Baret et al., 2013;Verger et al., 2014b) LAI products.

The FROM-GLC is the first global land cover product with 30 m spatial resolution (Gong et al., 2013), which is based on TM images and adopts images from MODIS and Google Earth as references. Due to the high resolution of 30 m, we used the latest version FROM-GLC-AGG (Yu et al., 2014) as the baseline PFT inputs. In addition, we mapped the land cover information of FROM-CLC to the PFTs mentioned in Table 1. The spatial resolution of the other two global land cover products, MODIS MCD12Q1 and CCI-LC, are 500 m and 300 m, and they are used to study the impact of the PFTs inputs. The PFTs proportions of three land cover products are illustrated in Table 3. The three products have the similar percentages of needleleaf trees, but the different percentages of the broadleaf trees, the CCI-LC has lower broadleaf trees cover rate compared with the other two products. Figure 2 shows the spatial distribution of the four main PFTs in model grids of LC products. As displayed by Figure 2, the three datasets present similar distributions, but various densities of forests. Because of the high emission factor of broadleaf trees, the highest broadleaf trees density of the MODIS LC data implies the highest emission density. Considering the high biomass and emission factor, the local broadleaf trees could lead to considerable emission potential. In contrast, the

distributions of shrub and grass have the bigger variances compared with those of trees, but the low emission factors limited their impacts on the estimation of terpenoids emission.

There are three different LAI datasets adopted in this study, and they are GLASS v1.1, MODIS MCD15 and GEO v2 LAI products, and three datasets have the same spatial resolution of 1 km. The temporal resolutions of GLASS and MODIS are both 8-days, and that of GEO v2 is 10-days. The GLASS v1.1 LAI products are retrieved from reprocessed Advanced Very High Resolution Radiometer (AVHRR) and MODIS reflectance data using the General Regression Neural Network (GRNN) (Xiao et al., 2014;Xiao et al., 2016), which was trained by the fused LAI from the MODIS and CYCLOPES LAI products. The GEO v1 adopts the Neural Network trained by the MODIS and CYCLOPES fused LAI to derive the LAI from the reflectance data from the SPOT/VEGETATION sensor (Baret et al., 2013). Based on GEO v1, the later GEO v2 employs a filtering approach to eliminate the outlier as well as the Savitzky-Golay and climatology temporal smoothing and gap filling methods to ensure consistency and continuity (Verger et al., 2014a). Due to the diverse satellite data sources and algorithms, these tree datasets are treated as dependent datasets and were used to study the impact of different satellite LAI inputs. Figure 3(a)-(c) show the spatial distribution of three LAI products in the model grid in summer. It should be noted that the MODIS MCD15 LAI product has a bigger mask area in the suburban and near water areas, which could directly lead to the loss of BVOC emissions in these areas. Although the satellite LAI values in suburban pixels have relatively high systematic error because of the mixed pixels (Jensen and Hardin, 2005), considering that the impact of the suburban or urban BVOC emissions may play a more important role in urban air quality, it is not a better solution to remove these pixels in this study. Figure 3(d) shows the monthly LAI values of three products. GEO v2 and GLASS have the similar lines and higher values from May to October than the MODIS LAI as shown in Figure 3(d). The peak LAI occurs in July for all three products, and mean LAI of three products during the winter seasons are all below 0.5 because of the low biomass of local deciduous tree species.

Table 4 presents the configurations of the simulation experiments. Because of the highest spatial resolution of the FROM LC product, the experiment using FROM PFT and GLASS LAI as inputs is the baseline experiment (E1). E1-E3 with the same PFT input and diverse LAI inputs are used to discover the impact of diverse LAI. In addition, the effect of PFT inputs is discovered by E1, E4 and E5 with same GLASS LAI input and different LC datasets. The meteorological conditions from WRF for MEGAN are processed by the MCIP tools (https://www.cmascenter.org/cmaq/).

3. Results and Description

MEGAN v2.1 can output 20 basic compounds, which could be divided into 150 VOC species (Guenther et al., 2012). And in this study, the VOC species are divided into four species as follows: isoprene, monoterpenes, sesquiterpenes and other VOCs. Monoterpenes include Myrcene, Sabinene, Limonene, 3-Carene, α-β-Ocimene, β-Pinene, α-Pinene, and other monoterpenes;

and the sesquiterpenes include α-Farnesene, β-Caryophyllene and other sesquiterpenes. We mainly discuss the terpenoids in the following sections because of their high reactivity as well as the larger uncertainties of other VOCs.

According to the baseline experiment (E1), the annual amount of BVOCs emission in Beijing of E1 is 99.9 Gg. As shown in pie chart of Figure 4, the proportions of isoprene, monoterpenes, sesquiterpenes and other VOCs are 52.6%, 11.1%, 1.4% and 34.9%, respectively. The isoprene, one of the most reactive species, accounts for over half of the total BVOCs. Table 5 presents the annual emissions of all experiments. E2 and E4 have relative approximate total emission amounts with E1 of 98.9 Gg and 94.9 Gg; and E3 and E5 decrease to 82.5 Gg and 74.0 Gg, with the percentages of 17.4% and 25.9% compared to the baseline, respectively. Comparing E1 with E2 and E3, the GEO LAI leads to less difference than the MODIS LAI on the total emission amounts. The decrease caused by the MODIS LAI is mainly due to the mask area and lower LAI value mentioned in Sec. 2.2.2. And according to Table 5, the impact of the GEO LAI on specific BVOC species are all lower than 3%. Considering the importance of the BVOCs emission in suburban areas on air quality, the GEO and GLASS LAI may be better choices in the BVOCs estimation for regional air quality simulation and forecasting.

As to the impact of the PFT inputs, E4 and E5 both lead to decrease with percentages of 5.0% and 25.9%, respectively. The decrease of E4 is against our prior estimation, that the large broadleaf trees cover rate of MODIS PFT dataset would lead to higher BVOCs emission. In addition, this result indicates that the standard emission factor is not the only decisive factor controlling the emission intensity and distribution.

Since the lookup table of the CCI-LC to convert the land cover index to the PFT index contains a scale factor to explain the mixed pixels, which increased the proportion of grass and decreased the proportions of other PFTs, and this prior process of CCI–LC leads to approximate a quarter in decrease for the total BVOCs amount as well as the specific species in E4. And in the E1-E3, the high spatial resolution (30 m) of FROM can diminish the mixed pixel problem of the MODIS (500 m) and CCI-LC (300 m) mesoscale sensor products in this study. The gap of the results between E1 and E5 emphasizes the significance of the accurate PFT in the BVOCs estimation under the MEGAN model frame, and the high-resolution vegetation species based map could help to diminish the uncertainty of PFTs when constructing local BVOCs inventory.

3.1 Temporal Variation of BVOCs in Beijing

As shown in Figure 4, the emission in summer are about 76.6% and that in winter are only about 0.3% of whole year BVOCs emission. Moreover, the ratio of BVOCs emissions between the summer and winter seasons is 239.46. Compared with the ratios of 9.77 (Wang et al., 2011) in the Pearl River Delta region and 4.9 (Leung et al., 2010) in Hong Kong, the temperate region exists the extremely large seasonal discrepancy of BVOCs emissions, and there is almost no BVOCs emission in winter owing to the low biomass of temperate deciduous trees (Stavrakou et al., 2014). In addition, high emission rates of BVOCs in summer imply the high potential risk of photochemistry pollution in summer considering the high temperature and radiation

conditions, and further investigation with the chemical transport model (CTM) is needed to analyze its impact on summer photochemical pollution.

Figure 5 shows the temporal variation of the four-separate species of all experiments, from E1 to E5. All experiments show a similar temporal distribution, and the peak value of all species appear in July, owing to the high biomass and the strong radiation intensity. Because of the low biomass and cold environment, all experiments have similar low emissions in winter-half year (from January to April and from October to December). And the emission values from May to September show obvious discrepancies, which indicates that the emission in summer contains more uncertainties. The ratios of four mains species between the highest (E1) and lowest experiment (E5) in July are 1.35, 1.36, 1.43 and 1.42, respectively, and the maximum difference is about 43%. The black lines represent the anterior estimated emissions of isoprene and monoterpenes in 1998 from Zhihui et al. (2003). As shown in Figure 5, all the results in this study are higher than the previous estimation. The ratio between E1 and results in Zhihui et al. (2003) of July are 6.8 and 3.19 for isoprene and monoterpenes respectively, and such ratios of the most conservative results (E5) still can reach 5.06 and 2.40. This huge gap between the two studies is due to multiple reasons. Firstly, we used the fully verified meteorological model outputs to replace the site observations, which could partly explain the gap between the two studies. On the other hand, Ghirardo et al. (2016) have reported that the BVOCs emission in megacity region of Beijing are doubled from year 2005 to 2010 according to the field surveys about the tree numbers. Moreover, the whole Beijing municipality, not only the urban part, also has the obvious development of the forest according to the local forest source surveys. Therefore, we considered that the development of local forest could be the main reason to explain the significant discrepancy of two studies. And under the background of global warming, it is reasonable to concern that the development of forest could enhance the natural impacts on the local air quality or the atmospheric environment(Penuelas and Staudt, 2010).

3.2 The Horizontal Distributions of BVOC emissions

Since the contribution of BVOCs in the summer season could reach 76.6% and the photochemistry is strong in summer, our analysis of horizontal distribution is mainly focused on the BVOCs emission in summer.

The spatial distribution of the correlation coefficient between the BVOCs and the main meteorological drivers is shown in Figure 6. Since a canopy model is adopted to calculate the leaf temperature of separated sunlit and shaded leaves by using DSW data, the isoprene and monoterpenes both show a strong correlation with DSW. Additionally, the light-dependent isoprene emission shows a more obvious correlation coefficient with DSW, and uneven distribution of DSW could directly affect the horizontal emission intensity of BVOCs, which means that the sunny slope may have a bigger emission potential than the shaded slope. Figure 7 displays the spatial distribution of the average emissions of four main VOC species during summer. E1, E2 and E3 present almost the same emission pattern of isoprene emissions with the same PFT inputs. As mentioned in Sec. 2.2.2, the mask area of the MODIS LAI directly leads to the missing value of BVOCs emissions in the

suburban area. Although the updating frequency of GLASS datasets is 8 days and that of GEO v2 is 10 days, E1 and E2 have almost the same spatial distribution. Comparing E4 and E5 with the baseline, conspicuous spatial variance can be found, which is mainly led by the distribution and density of broadleaf trees, the PFT species with the highest emission potential. E5, with CCI land cover, has the lowest emission intensity of isoprene because of the low density of broadleaf trees. The MODIS LC products have the highest broadleaf trees cover rate (Figure 2); however, these regions do not show the obvious high emission intensity of isoprene in E4 because of the limitation of meteorological conditions. According to the of E1, the main emission pools of isoprene are the west and the northeast region to the megacity area. Although the forest area is lacking NOx emissions, the oxides of isoprene, e.g., formaldehyde, could affect city air quality by transporting to the city region (Geng et al., 2011); meanwhile, the NOx from the urban area could transport to the rural area and form O_3.

Spatial distributions of the monoterpenes and sesquiterpenes in the Beijing region are also displayed in Figure 7. Except of the impact of broadleaf trees, the spatial distribution of needleleaf trees also affects the horizontal pattern of monoterpenes and sesquiterpenes. The comparison of E1 and E2 illustrates the limited impact of LAI inputs on estimation of monoterpene and sesquiterpene emissions.

3.3 The Roles of Different PFTs of BVOC Emissions in Beijing

To investigate the contribution of every PFT, we set all PFTs to zero, except for the one that needs to be investigated (Sakulyanontvittaya et al., 2008). According to their relatively low contribution, herbaceous species are merged into one main species, and four species, including broadleaf trees, needleleaf trees, shrub, and “crop & grass”, are used to statistically analyse the contribution. Indicated by Figure 8, broadleaf trees contribute 94.5% isoprene, 53.3% monoterpenes, 53.8% sesquiterpenes and 34.1% other VOCs; overall, the broadleaf trees contribute 68.3% of BVOCs emissions. And the broadleaf trees play the most significant role in BVOC emissions in Beijing, since the broadleaf trees occupy 27.3% of the local area according to FROM products; at the same time, broadleaf trees also have the highest emission potential and biomass (Zhihui et al., 2003). The shrub contributes 24.9% monoterpenes and 23.1% sesquiterpenes, and because of the limitation of the emission potential in Table 1, it only contributes 2.3% isoprene. The needleleaf trees occupy 7.3% of the local area, but have the obvious monoterpene and sesquiterpene emission contributions of 20.8% and 18.7%, respectively. Crop and grass occupied 39.1% of the local land area according to Table 3; however, because of their low emission potential for terpenoids (Guenther et al., 2006), they only contribute 3.0% isoprene, 1.0% monoterpenes, and 4.4% sesquiterpenes. In contrast, grass and crop contribute 42.83% of other VOCs, which is due to the large-scale distribution, but the results of other VOCs have large uncertainty due to complex species and unmeasured emission factors.

3.4 Discussion

Table 6 presents the estimated BVOCs emission in Beijing in this study and previous studies, and the total emissions (Gg) are converted into the area average emission intensity (g/m^2) for comparing conveniently. The results in this study of isoprene and monoterpenes are higher than the results in Zhihui et al. (2003), as well as Klinger et al. (2002), but close to the results of year 2010 in Ghirardo et al. (2016). The ratio of isoprene between our results and Zhihui et al. (2003) as well as Klinger et al. (2002) are 5.92 and 3.33, and the ratio of monoterpenes between our results and Zhihui et al. (2003) and Klinger et al. (2002) are 2.83 and 1.26, respectively. On one hand, the broadleaf and needleleaf forest cover rates in Zhihui et al. (2003) are 5% and 2%, which are 27.3% and 7.3% in this study, respectively. The ratios of forest area of two studies are 5.47 and 3.66 for the broadleaf trees and needleleaf trees, respectively, which are similar to the emission ratios of isoprene (5.92) and monoterpenes (2.83) between the two studies. Therefore, the change of forest area could be the main reason accounting for the gap between the two studies.

Moreover, the forest coverage rate in Beijing keeps rising under the greening policy, and the investigation results from the NFRS indicates that the forest coverage rate increased from 20.6% to 35.8% during 1998-2013 in Beijing. The increasing forest coverage rate, especially the tree species with high BVOC emission potential, e.g., *Quercus* and *Populus,* would increase the impact of BVOCs on the local atmospheric chemistry balance and air quality, especially ozone pollution. Ghirardo et al. (2016) also had the similar concern and conclusion, and choosing low emission potential tree species should be considered and added into the strategy of local greening work.

3.5 Uncertainties

In this study, the uncertainties mainly focus on the satellite inputs of the model, the meteorological inputs and the standard emission factors.

For the LAI input, we adopted three independent LAI satellite datasets to study its effect. The results show that, except for the MODIS LAI product, the GLASS LAI and GEO LAI could lead to relative small difference for the total emissions, and the temporal and horizontal differences have been discussed in Sec. 3.2 and 3.4. Overall, the impact of the satellite LAI input is limited under the model frame of MEGAN.

On the one hand, the standard emission factor of isoprene in this study comes from previous publications (Zhihui et al., 2003;Klinger et al., 2002), and we adopted the area data of tree species from the 7^{th} NFRS to distribute the emission factors of the PFTs. Although previous studies (Zhihui et al., 2003;Ghirardo et al., 2016) have provided the partial BVOC emission factors, more field investigations are needed to provide the emission factors of local tree species and validate the model. On the other hand, the PFT distribution directly decides the emission ability and spatial distribution of sources, and we used three different land cover datasets to learn the impact of PFT inputs. The results demonstrate that local BVOC emissions are sensitive

to the PFT inputs, and the diverse PFT inputs lead to the different total emissions, as well as the spatial distributions, and the accurate PFT or LC input is helpful to constrain the uncertainty of BVOC emissions.

The meteorological conditions decide the temporal variance of the BVOCs emission. Because of the lack of observations, especially the radiation observation, the meteorological model results could be more reasonable to explain the spatial difference of the high resolution BVOCs emission inventory, but the systematic error from the deficiency of aerosol extinction and the simulation bias of clouds could directly lead to the overestimation of BVOCs emissions (Wang et al., 2011).

4. Conclusion and future work

To investigate the contribution of natural emissions on local air quality, the first step is to estimate the reliable BVOCs emission inventory. This work established an hourly, 3-km gridded inventory of BVOCs emissions over Beijing in 2013 based on the latest MEGAN 2.1 model. MEGAN model was driven by WRF v3.3.1 model, and diverse satellite LAIs and PFTs were adopted to investigate and constrain the uncertainties of input variables. Because of the highest spatial resolution of FROM LC product, the results of experiment with FROM LC and GLASS LAI datasets are treated as the baseline results.

(1) According to the estimation of the baseline experiment, the total amount of BVOCs is 99.9 Gg in Beijing in 2013, and isoprene, monoterpenes, sesquiterpenes and other VOCs account for 52.6%, 11.1%, 1.4% and 34.9% of the local BVOCs emission, respectively.

(2) The summer season contributes 76.6% of the BVOC emissions in Beijing, and winter only contributes 0.3% BVOCs emissions because of the low temperature and near-zero biomass of deciduous trees. Considering the high temperature and radiation situation in summer, the high BVOCs emission could affect the local photochemical chemistry, and the regional CTM will be used to investigate and evaluate the role of BVOCs on local air pollution as the next step research.

(3) The broadleaf trees account for 68.3% of the total BVOC emissions over Beijing. On the one hand, the broadleaf trees play an important role in Beijing since they occupy 27.3% local area according to FROM products; on the other hand, broadleaf trees have the highest emission potential and biomass (Zhihui et al., 2003), and such features of local broadleaf forest make it dominate the local BVOCs emission.

(4) Different satellite LAI inputs were adopted to investigate the impact of LAI. MODIS LAI led to a 17.4% decline of total BVOCs compared with baseline in this study, because of the relative big mask area in MODIS LAI product. The variance of GEO and GLASS LAI products only led to 1.0% difference of total BVOCs emission, and the differences of each BVOC species are lower than 3.0% at the same time with similar spatial and temporal distributions. Generally, the uncertainty of LAI is limited under the MEGAN model frame, and the GEO and GLASS LAI products could be the better choices for regional BVOC emissions estimation compared with the MODIS LAI, which would lead to the missing emissions of the suburban area.

(5) The FROM-AGG, MODIS MCD12Q1 and CCI-LC land cover products are adopted to investigate the sensitivity of the model to land cover data. Although MODIS LC has the highest broadleaf cover rate of 30.3%, it led to 5% decline of total BVOCs emission because of the influence of spatial distribution of meteorological conditions. The CCI-LC would lead to a sharp decline of 26.0% of total BVOCs emissions, owing to the relatively low cover percentage of forest in Table 3.

(6) The estimated emission of BVOCs in this study is much higher than that of earlier estimations (Zhihui et al., 2003;Klinger et al., 2002) and is similar to a recent study of the megacity area (Ghirardo et al., 2016). The development of forest areas is main reason to explain the gap between this study and earlier results, which is familiar with the conclusion derived by Ghirardo et al. (2016). With the development of local forests, the BVOCs would play a more important role in local atmospheric environment.

Acknowledgements.

The National Key R&D Program of China (2017YFC0209805), the National Natural Science Foundation of China (41305121) and the Fundamental Research Funds for the Central Universities funded this work.

References

Arneth, A., Niinemets, Ü., Pressley, S., Bäck, J., Hari, P., Karl, T., Noe, S., Prentice, I., Serça, D., and Hickler, T.: Process-based estimates of terrestrial ecosystem isoprene emissions: incorporating the effects of a direct CO 2-isoprene interaction, Atmospheric Chemistry and Physics, 7, 31-53, 2007.

Baret, F., Weiss, M., Lacaze, R., Camacho, F., Makhmara, H., Pacholcyzk, P., and Smets, B.: GEOV1: LAI and FAPAR essential climate variables and FCOVER global time series capitalizing over existing products. Part1: Principles of development and production, Remote Sensing of Environment, 137, 299-309, https://doi.org/10.1016/j.rse.2012.12.027, 2013.

Carlton, A. G., and Baker, K. R.: Photochemical modeling of the Ozark isoprene volcano: MEGAN, BEIS, and their impacts on air quality predictions, Environ Sci Technol, 45, 4438-4445, 10.1021/es200050x, 2011.

Claeys, M., Graham, B., Vas, G., Wang, W., Vermeylen, R., Pashynska, V., Cafmeyer, J., Guyon, P., Andreae, M. O., and Artaxo, P.: Formation of secondary organic aerosols through photooxidation of isoprene, Science, 303, 1173-1176, 2004.

Emmons, L. K., Walters, S., Hess, P. G., Lamarque, J. F., Pfister, G. G., Fillmore, D., Granier, C., Guenther, A., Kinnison, D., and Laepple, T.: Description and evaluation of the Model for Ozone and Related chemical Tracers, version 4 (MOZART-4), Geoscientific Model Development, 3, 43-67, 2010.

Fuentes, J. D., Lerdau, M., Atkinson, R., Baldocchi, D., Bottenheim, J. W., Ciccioli, P., Lamb, B., Geron, C., Gu, L., and Guenther, A.: Biogenic Hydrocarbons in the Atmospheric Boundary Layer: A Review, Bulletin of the American Meteorological Society, 81, 1537-1576, 2000.

Geng, F., Tie, X., Guenther, A., Li, G., Cao, J., and Harley, P.: Effect of isoprene emissions from major forests on ozone formation in the city of Shanghai, China, Atmospheric Chemistry and Physics, 11, 10449-10459, 10.5194/acp-11-10449-2011, 2011.

Ghirardo, A., Xie, J., Zheng, X., Wang, Y., Grote, R., Block, K., Wildt, J., Mentel, T., Kiendler-Scharr, A., Hallquist, M., Butterbach-Bahl, K., and Schnitzler, J.-P.: Urban stress-induced biogenic VOC emissions and SOA-forming potentials in Beijing, Atmospheric Chemistry and Physics, 16, 2901-2920, 10.5194/acp-16-2901-2016, 2016.

Gong, P., Wang, J., Yu, L., Zhao, Y., Zhao, Y., Liang, L., Niu, Z., Huang, X., Fu, H., Liu, S., Li, C., Li, X., Fu, W., Liu, C., Xu, Y., Wang, X., Cheng, Q., Hu, L., Yao, W., Zhang, H., Zhu, P., Zhao, Z., Zhang, H., Zheng, Y., Ji, L., Zhang, Y., Chen, H., Yan, A., Guo, J., Yu, L., Wang, L., Liu, X., Shi, T., Zhu, M., Chen, Y., Yang, G., Tang, P., Xu, B., Giri, C., Clinton, N.,

Zhu, Z., Chen, J., and Chen, J.: Finer resolution observation and monitoring of global land cover: first mapping results with Landsat TM and ETM+ data, International Journal of Remote Sensing, 34, 2607-2654, 10.1080/01431161.2012.748992, 2013.

Guenther, A., Hewitt, C. N., Erickson, D., Fall, R., Geron, C., Graedel, T., Harley, P., Klinger, L., Lerdau, M., McKay, W. A., Pierce, T., Scholes, B., Steinbrecher, R., Tallamraju, R., Taylor, J., and Zimmerman, P.: A global model of natural volatile organic compound emissions, Journal of Geophysical Research, 100, 8873, 10.1029/94jd02950, 1995.

Guenther, A., Baugh, B., Brasseur, G., Greenberg, J., Harley, P., Klinger, L., Serça, D., and Vierling, L.: Isoprene emission estimates and uncertainties for the central African EXPRESSO study domain, Journal of Geophysical Research: Atmospheres, 104, 30625-30639, 10.1029/1999jd900391, 1999.

Guenther, A., Karl, T., Harley, P., Wiedinmyer, C., Palmer, P., and Geron, C.: Estimates of global terrestrial isoprene emissions using MEGAN (Model of Emissions of Gases and Aerosols from Nature), Atmos. Chem. Phys, 6, 3181-3210, 2006.

Guenther, A. B., Jiang, X., Heald, C. L., Sakulyanontvittaya, T., Duhl, T., Emmons, L. K., and Wang, X.: The Model of Emissions of Gases and Aerosols from Nature version 2.1 (MEGAN2.1): an extended and updated framework for modeling biogenic emissions, Geoscientific Model Development, 5, 1471-1492, 10.5194/gmd-5-1471-2012, 2012.

Jensen, R. R., and Hardin, P. J.: Estimating urban leaf area using field measurements and satellite remote sensing data, Journal of Arboriculture, 31, 21-27, 2005.

Kavouras, I. G., Mihalopoulos, N., and Stephanou, E. G.: Formation of atmospheric particles from organic acids produced by forests, Nature, 395, 683-686, 1998.

Klinger, L. F., Li, Q. J., Guenther, A. B., Greenberg, J. P., Baker, B., and Bai, J. H.: Assessment of volatile organic compound emissions from ecosystems of China, Journal of Geophysical Research: Atmospheres, 107, ACH 16-11-ACH 16-21, 10.1029/2001jd001076, 2002.

Leung, D., Wong, P., Cheung, B., and Guenther, A.: Improved land cover and emission factors for modeling biogenic volatile organic compounds emissions from Hong Kong, Atmospheric Environment, 44, 1456-1468, 2010.

Makkonen, R., Asmi, A., Kerminen, V. M., Boy, M., Arneth, A., Guenther, A., and Kulmala, M.: BVOC-aerosol-climate interactions in the global aerosol-climate model ECHAM5.5-HAM2, Atmospheric Chemistry and Physics, 12, 10077-10096, 10.5194/acp-12-10077-2012, 2012.

Penuelas, J., and Staudt, M.: BVOCs and global change, Trends Plant Sci, 15, 133-144, 10.1016/j.tplants.2009.12.005, 2010.

Safieddine, S., Boynard, A., Hao, N., Huang, F., Wang, L., Ji, D., Barret, B., Ghude, S. D., Coheur, P.-F., Hurtmans, D., and Clerbaux, C.: Tropospheric ozone variability during the East Asian summer monsoon as observed by satellite (IASI), aircraft (MOZAIC) and ground stations, Atmospheric Chemistry and Physics, 16, 10489-10500, 10.5194/acp-16-10489-2016, 2016.

Sakulyanontvittaya, T., Duhl, T., Wiedinmyer, C., Helmig, D., Matsunaga, S., Potosnak, M., Milford, J., and Guenther, A.: Monoterpene and sesquiterpene emission estimates for the United States, Environmental science & technology, 42, 1623-1629, 2008.

Seinfeld, J. H., and Pandis, S. N.: Atmospheric Chemistry and Physics: From Air Pollution to Climate Change, 2nd Edition, 2012.

Skamarock, W. C., Klemp, J. B., Dudhia, J., Gill, D. O., Barker, D. M., Wang, W., and Powers, J. G.: A description of the advanced research WRF version 2, DTIC Document, 2005.

Stavrakou, T., Müller, J. F., Bauwens, M., De Smedt, I., Van Roozendael, M., Guenther, A., Wild, M., and Xia, X.: Isoprene emissions over Asia 1979-2012: impact of climate and land-use changes, Atmospheric Chemistry and Physics, 14, 4587-4605, 10.5194/acp-14-4587-2014, 2014.

Tie, X., Li, G., Ying, Z., Guenther, A., and Madronich, S.: Biogenic emissions of isoprenoids and NO in China and comparison to anthropogenic emissions, Science of the total environment, 371, 238-251, 2006.

Verger, A., Baret, F., and Weiss, M.: Near Real-Time Vegetation Monitoring at Global Scale, IEEE Journal of Selected Topics in Applied Earth Observations and Remote Sensing, 7, 3473-3481, 10.1109/JSTARS.2014.2328632, 2014a.

Verger, A., Baret, F., Weiss, M., Smets, B., Camacho, F., and Lacaze, R.: GEOV2/VGT: Near real time estimation of LAI, FAPAR and cover fraction variables from VEGETATION data within Copernicus Global Land service, Fourth International Symposium on Recent Advances in Quantitative Remote Sensing, Valence, Spain, 2014, 2014b.

Wang, J.-L., Chew, C., Chang, C.-Y., Liao, W.-C., Lung, S.-C. C., Chen, W.-N., Lee, P.-J., Lin, P.-H., and Chang, C.-C.: Biogenic isoprene in subtropical urban settings and implications for air quality, Atmospheric Environment, 79, 369-379, 10.1016/j.atmosenv.2013.06.055, 2013.

Wang, T., Ding, A., Gao, J., and Wu, W. S.: Strong ozone production in urban plumes from Beijing, China, Geophysical Research Letters, 33, 10.1029/2006gl027689, 2006.

Wang, X., Situ, S., Guenther, A., Chen, F. E. I., Wu, Z., Xia, B., and Wang, T.: Spatiotemporal variability of biogenic terpenoid emissions in Pearl River Delta, China, with high-resolution land-cover and meteorological data, Tellus B, 63, 241-254, 10.1111/j.1600-0889.2010.00523.x, 2011.

Xiao, Z., Liang, S., Wang, J., Chen, P., Yin, X., Zhang, L., and Song, J.: Use of General Regression Neural Networks for Generating the GLASS Leaf Area Index Product From Time-Series MODIS Surface Reflectance, IEEE Transactions on Geoscience and Remote Sensing, 52, 209-223, 10.1109/tgrs.2013.2237780, 2014.

Xiao, Z., Liang, S., Wang, J., Xiang, Y., Zhao, X., and Song, J.: Long-Time-Series Global Land Surface Satellite Leaf Area Index Product Derived From MODIS and AVHRR Surface Reflectance, IEEE Transactions on Geoscience and Remote Sensing, 54, 5301-5318, 10.1109/tgrs.2016.2560522, 2016.

Yu, L., Wang, J., Li, X., Li, C., Zhao, Y., and Gong, P.: A multi-resolution global land cover dataset through multisource data aggregation, Science China Earth Sciences, 57, 2317-2329, 10.1007/s11430-014-4919-z, 2014.

Zhao, C., Wang, Y., Yang, Q., Fu, R., Cunnold, D., and Choi, Y.: Impact of East Asian summer monsoon on the air quality over China: View from space, Journal of Geophysical Research Atmospheres, 115, 1063-1063, 2010.

Zhihui, W., Yuhua, B., and Shuyu, Z.: A biogenic volatile organic compounds emission inventory for Beijing, Atmospheric environment, 37, 3771-3782, 2003.

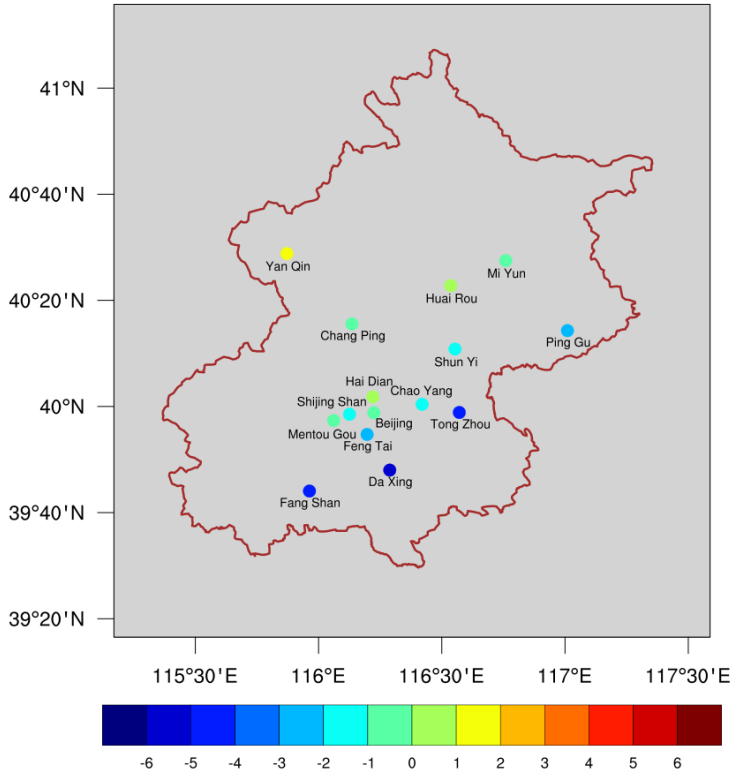

Figure 1. Spatial distribution of the MB of T2 from all available sites.

Atmos. Chem. Phys. Discuss., https://doi.org/10.5194/acp-2017-945
Manuscript under review for journal Atmos. Chem. Phys.
Discussion started: 15 December 2017

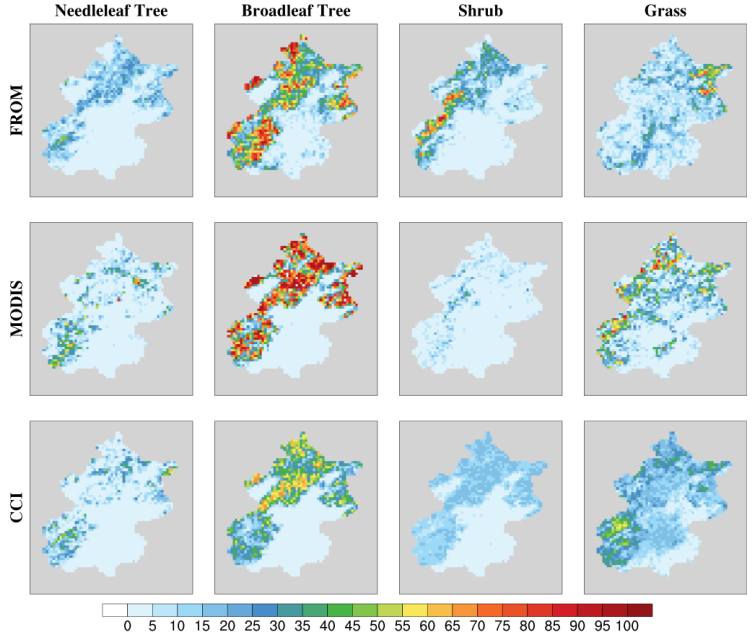

Figure 2. Spatial distribution of the proportions of PFTs in model grids from three land cover inputs.

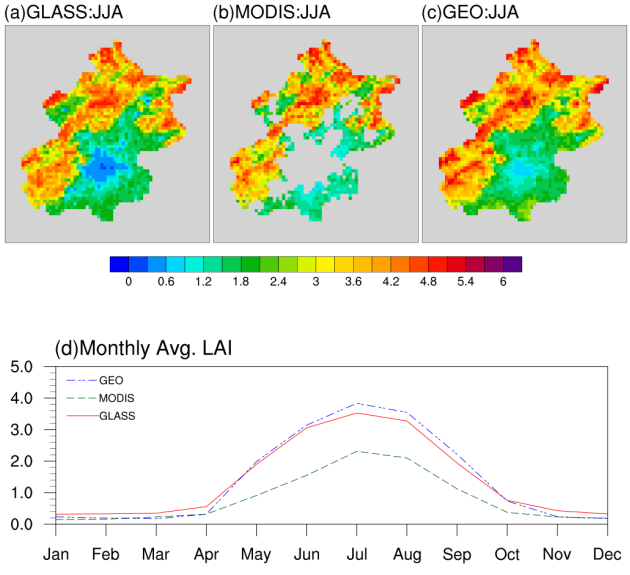

Figure 3. (a)-(c) show the average spatial distribution of GLASS, MODIS and GEO v2 LAI in the summer season, and (d) shows the monthly LAI values of the above products with the same masking area.

Atmos. Chem. Phys. Discuss., https://doi.org/10.5194/acp-2017-945
Manuscript under review for journal Atmos. Chem. Phys.
Discussion started: 15 December 2017

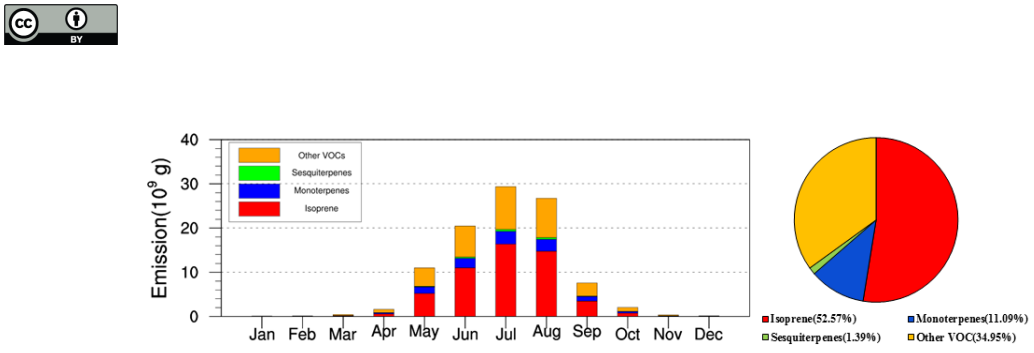

Figure 4. The temporal variability of BVOCs emissions over Beijing in 2013, and the proportions of each main species.

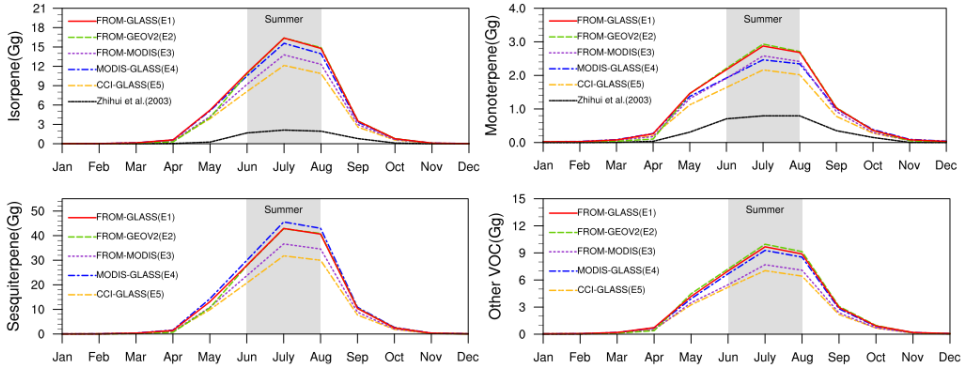

Figure 5. The temporal variability of BVOCs of all simulation experiments.

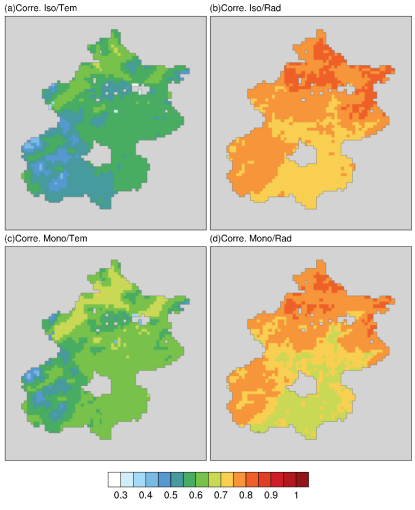

Figure 6. The spatial distribution of the correlation coefficient between main meteorological drivers and BVOCs emissions. (a) and (b) are the correlation coefficients between the isoprene emission and air temperature and DSW, respectively; and (c) and (d) display the correlation coefficients between the monoterpene emission and air temperature and DSW, respectively.

Atmos. Chem. Phys. Discuss., https://doi.org/10.5194/acp-2017-945
Manuscript under review for journal Atmos. Chem. Phys.
Discussion started: 15 December 2017

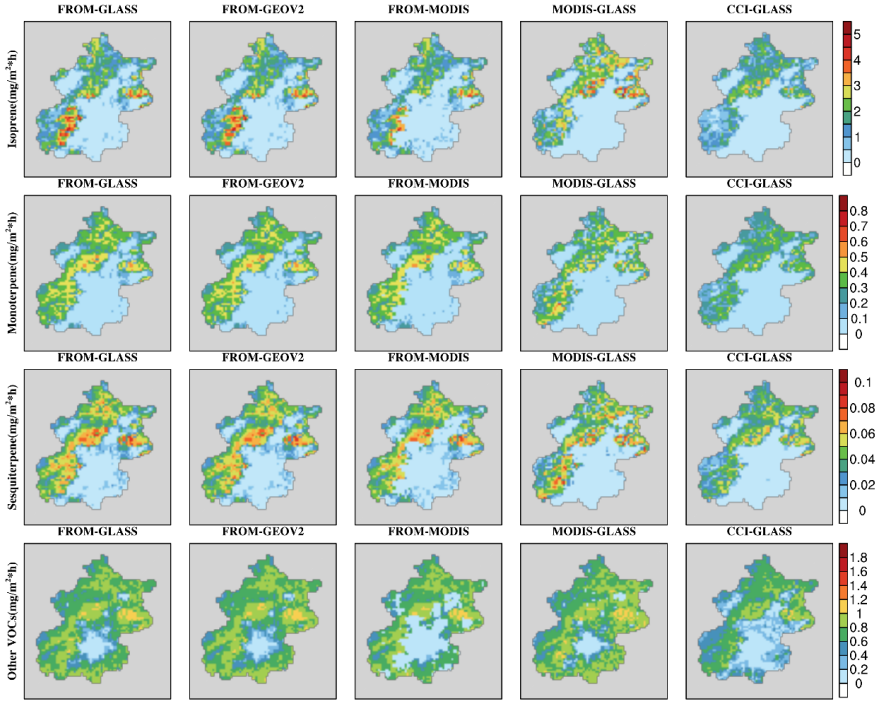

Figure 7. The spatial distribution of average emissions of four main VOC species in summer.

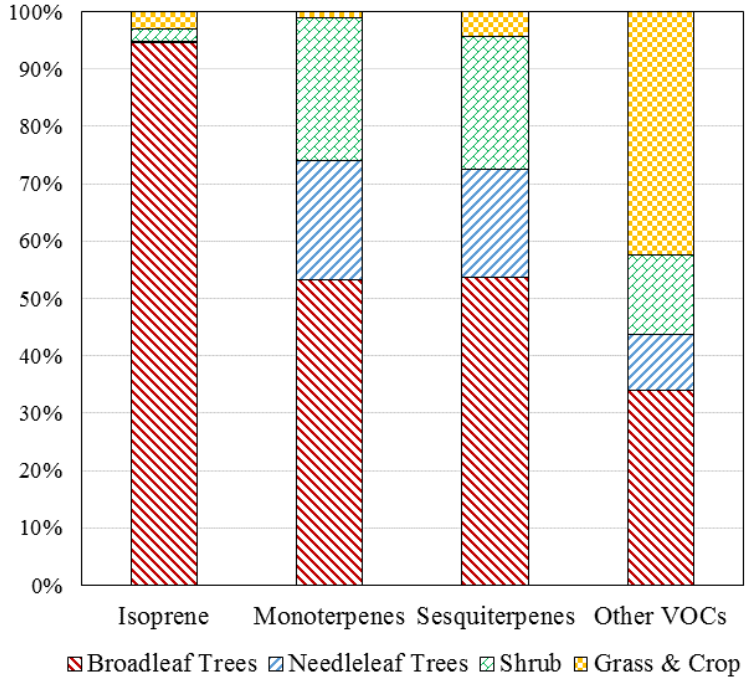

Figure 8. The contribution of different PFT species to the different BVOC species in E1.

Atmos. Chem. Phys. Discuss., https://doi.org/10.5194/acp-2017-945
Manuscript under review for journal Atmos. Chem. Phys.
Discussion started: 15 December 2017

Atmospheric Chemistry and Physics Discussions

Table 1. Adjusted (original) isoprene emission factors for each PFT.

PFT	Broadleaf Trees	Needleleaf Trees	Shrub	Grass	Cereal Crop	Corn
EF (μg /m^2 ·h)	11736 (10000)	94 (600)	712 (4000)	800 (800)	50 (50)	1 (1)

Table 2. Statistics of the primary verification of the temperature (T2) with in situ data. The ME, MB and RMSE are abbreviations for mean error, mean bias and root mean square error, respectively.

Name	ME	MB	R	RMSE
Beijing	1.97	-0.2	0.97	2.48
Hai Dian	1.91	0.01	0.97	2.46
Chao Yang	2.27	-1.15	0.96	2.82
Shun Yi	2.17	-1.4	0.97	2.77
Huai Rou	1.98	0.19	0.97	2.51
Tong Zhou	4.86	-4.84	0.97	5.44
Chang Ping	2.12	-0.49	0.97	2.67
Yan Qin	2.84	1.81	0.96	3.46
Feng Tai	2.65	-2.07	0.96	3.34
Shijing Shan	2.2	-1.07	0.96	2.81
Da Xing	5.13	-5.11	0.96	5.8
Fang Shan	4.56	-4.5	0.96	5.34
Mi Yun	2.1	-0.46	0.96	2.73
Mengtou Gou	2.06	-0.56	0.96	2.64
Ping Gu	2.95	-2.61	0.97	3.7
Mean	2.78	-1.50	0.96	3.40

Table 3. The percentage of different PFT areas in Beijing from three LC datasets

	Broadleaf Trees	Needleleaf Trees	Shrub	Grass	Crop	Corn
FROM-AGG	27.3%	7.3%	11.3%	11.9%	27.2%	15.0%
MODIS LC	30.3%	6.6%	2.3%	15.8%	33.3%	11.7%
CCI-LC	20.0%	6.3%	8.4%	16.6%	13.4%	35.3%

Table 4. The configurations of simulation experiments. E1 is the baseline experiment, and E1-E3 are used to discover the impact of LAI inputs. The impact of different PFT inputs are discovered by E1, E4 and E5.

	Land Cover	Leaf Area Index
E1 (Baseline)	FROM	GLASS v1.1
E2	FROM	GEO v2
E3	FROM	MODIS MCD15
E4	MODIS MCD12Q1	GLASS v1.1

E5	CCI-LC	GLASS v1.1

Table 5. The totally annual BVOC emissions of all experiments.

	Isoprene (Gg)	Monoterpenes (Gg)	Sesquiterpenes (Gg)	Other VOCs (Gg)	SUM (Gg)
E1	52.5	11.1	1.4	34.9	99.9
E2	50.9	11.0	1.4	35.6	98.9
E3	43.8	9.8	1.2	27.7	82.5
E4	50.1	10.0	1.5	33.3	94.9
E5	38.8	8.4	1.0	25.8	74.0

Table 6. Comparison of the average emission intensities of isoprene and monoterpenes from this study and previous publications.

	Year	Area (km^2)	Isoprene (g/m^2)	Monoterpenes (g/m^2)
Zhihui et al. (2003)	1998	16400	0.54	0.24
Klinger et al. (2002)	2002	16400	0.96	0.54
Ghirardo et al. (2016)	2005 (city level)	1434	1.81	0.28
Ghirardo et al. (2016)	2010 (city level)	1434	3.70	0.56
This Study	2013	16400	2.4-3.2	0.51-0.68